JOURNAL OF MATERIALS SCIENCE 29 (1994) 4306–4313

Effect of mechanical deformation and annealing on the evolution of *c*-axis texture of $Bi_{1.6}Pb_{0.4}Sr_2Ca_2Cu_3O_z$ superconductor hot-isostatic-press cladded onto a Ag substrate

J. M. YOO, K. MUKHERJEE
Department of Materials Science and Mechanics, Michigan State University, East Lansing, MI 48824, USA

A systematic study was undertaken of the mechanical deformation and annealing effects on the *c*-axis texture evolution of a $Bi_{1.6}Pb_{0.4}Sr_2Ca_2Cu_3O_z$ (BSCCO) superconductor cladded onto a Ag substrate. As the amount of cold-rolling reduction (%) increased, a tighter clustering of the $(00\underline{1}\,\underline{4})$ poles around the surface normal indicated that randomly oriented grains from the initial hot-isostatic-press (HIP) cladded surface are progressively oriented nearly perpendicularly to the plane of the tape. Conventional X-ray diffraction (XRD), and X-ray pole-figure studies support a basal-plane sliding mechanism of plastic deformation. In samples annealed for 100 h, the superconductor (BSCCO) material near the BSCCO/Ag interface appears to undergo incipient melting, and there is a layer-like growth (*c*-axis texture), which extends macroscopically from the Ag interface. The sample-orientation distribution of short-term (5 h) annealed samples showed a strong *c*-axis texture, with the *c*-axis aligned nearly perpendicularly to the plane of the tape with no preferred alignment of the *a*- and *b*-axes.

1. Introduction

In recent years, much research has focused on the processing techniques of high-T_c superconductor materials in the form of wire or tape for high-current and high-field applications [1–3]. The fabrication of tapes or wires from these ceramics is an extremely challenging task, since the processing must lead to chemically and mechanically optimized microstructures if these tapes are to transport large current densities in high magnetic fields.

The achievement of such ideal microstructures depends upon fulfilling: (i) a crystallographic texture characterized by a high degree of alignment of the superconducting crystal planes lying parallel to the conducting direction, (ii) a high degree of densification, and (iii) a minimal volume percentage of the second phase. The need for strong microstructural control is dictated by the intrinsic anisotropic properties of these materials, resulting from anisotropic crystal structures.

Our research focused on Bi–Sr–Ca–Cu–O systems with the major emphasis on the $Bi_{1.6}Pb_{0.4}Sr_2Ca_2Cu_3O_z$ compound, known as 2223 (BSCCO) because of its high critical temperature. For these compounds, there is now a convincing body of experimental evidence which shows that a strong crystallographic texture is essential to minimize weak links and to achieve a high critical current density. For example, for 2212 (BSCCO) tapes, Enomoto *et al.* [4] found that the critical current density increased sharply as the degree of *c*-axis texture of their tapes increased. A similar result has been reported for 2223 (BSCCO) tapes by Jin *et al.* [5]. Those *c*-plane grain boundaries which have large misorientations are also reported to decrease the critical current density [6].

An important, and as yet little understood, area is the relationship between thermomechanical treatment and grain alignment in this class of superconductor materials. The exact mechanism for texture formation in the silver-clad BSCCO tape during the rolling and annealing process is not clearly described in the literature. Consequently, a systematic study was undertaken by us to investigate the effect of mechanical deformation and annealing on the *c*-axis texture of a $Bi_{1.6}Pb_{0.4}Sr_2Ca_2Cu_3O_z$/Ag composite compacted by HIP-cladding technique. We analysed the effect of thermomechanical treatment, involving rolling and annealing, on the *c*-axis-texture development.

It is very difficult, using a conventional process, to clad high-T_c BSCCO superconductors on a Ag substrate due to the very narrow sintering-temperature range [7], without decomposition of the high-T_c phase. In order to obtain good BSCCO/Ag interface bonding, and high-density BSCCO layers prior to rolling, we used hot-isostatic-press (HIP) technique to clad a BSCCO superconductor on Ag. In addition, our previous results [8] show good stability of the

0022–2461

BSCCO superconductor with respect to oxygen stoichiometry during HIP processing.

2. Experimental procedure

The 2223 BSCCO/Ag superconducting tape was fabricated in several processing steps. High-purity (> 99.9%) oxides or carbonates of Bi, Pb, Sr, Ca and Cu, with a cation ratio of 1.6:0.4:2.0:2.0:3.0, were carefully mixed, heat calcined and reground. The high-T_c-phase powder thus prepared was first compacted into a cylindrical shape by uniaxial compression. The next step was HIP consolidation. Multilayer stacks consisting of alternate layers of 2223 (BSCCO) and silver were coated with a BN spray and encapsulated in a Pyrex tube under vacuum prior to HIP consolidation.

As shown in the schematic diagram in Fig. 1, the sealed samples were HIP processed in an Ar atmosphere at a temperature of 850 °C, at a pressure of 138 MPa for 3 h to obtain high-density BSCCO layers. These samples also exhibited a good BSCCO/Ag-interface bonding strength prior to rolling. The hot-isostatic-pressed (HIPed) samples were cooled slowly at a rate of 100 °C h^{-1}. Pre-forms for the cold-rolling process were cut from these multilayer stacks. BSCCO/Ag-composite tape was obtained by cold rolling using multiple passes and intermediate annealing.

The phase identification and crystal structure determination were performed using a Scintag-XDS-200 X-ray diffractometer, equipped with a computerized data-collection system. The texture analysis was also performed by using a Scintag pole-figure goniometer, equipped with a popLA software package. The preferred-orientation-package Los Alamos (popLA) package is a comprehensive, coherent, menu-driven set of utility programs that is independent of the texture-measurement hardware [9]. The critical current density was measured at 77 K, using a four-probe technique. Microstructural and compositional studies were performed using a Hitachi S-2500C scanning electron microscope equipped with a Link energy dispersive spectrometer.

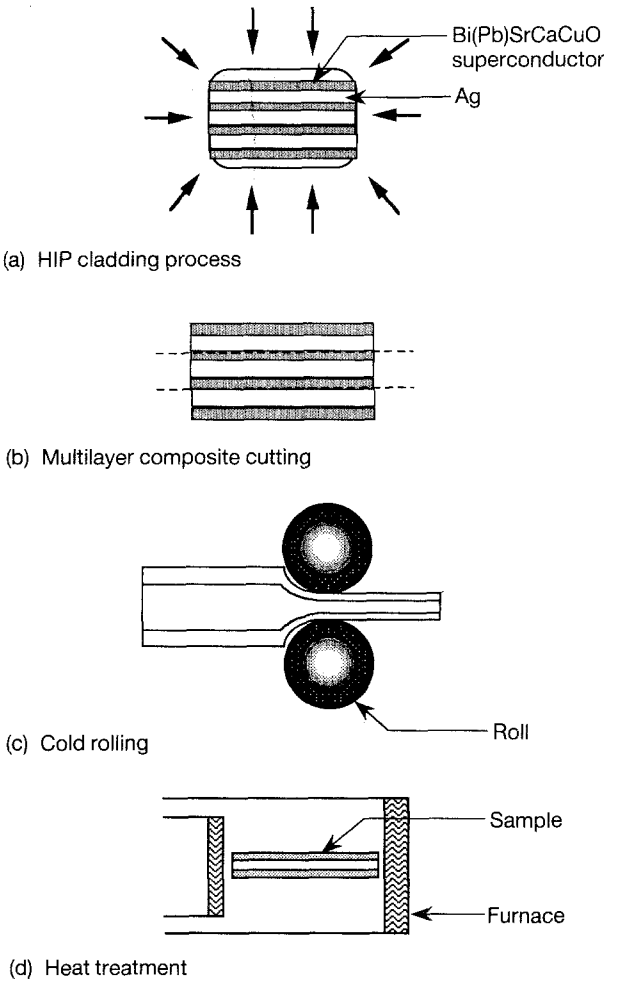

Figure 1 A schematic illustration of the processing steps for the BSCCO/Ag-superconductor tape.

3. Results and discussion

XRD studies of the BSCCO/Ag tape produced by an oxide-powder-in-tube (OPIT) technique [1, 2] have been widely used to investigate the *c*-axis alignment. However, one concern is that the X-ray penetration depth for CuK_α radiation is only a few micrometres. Since the most common method of exposing the BSCCO layer produced by the powder-in-tube method is to grind off one side of the Ag cladding, the exposed layer generally lies close to the Ag–BSCCO interface, where the alignment is greatest [10]. These XRD measurements will consequently tend to overestimate the overall *c*-axis grain alignment of all samples and will minimize the differences between samples.

In our experiments, however, without peeling off the silver, directly rolled surfaces were studied by X-ray diffractometry and pole-figure goniometry. Even then, the X-ray-penetration-depth problem cannot be excluded. Fig. 2 shows the measured XRD data for a successively cold-rolled sample as a function of the cold-rolling thickness reduction (%). After the HIP-cladding process, the surface of a sample contains numerous XRD peaks, such as (1 1 5), (1 1 9), (2 0 0), and (1 1 $\underline{1}$ $\underline{1}$), along with the desirable (0 0 1) peak. The (0 0 $\underline{1}$ 0), (0 0 $\underline{1}$ 4) peak intensities increased while the (1 1 5), (2 0 0), (1 1 9), and (1 1 $\underline{1}$ $\underline{1}$) peak intensities decreased after 20% cold rolling. Intensities other than (0 0 1) decreased consistently with the amount of cold-rolling reduction. After 95% cold-rolling, the (1 1 5) peak intensity almost disappeared, and very little trace of (1 1 9) or (1 1 $\underline{1}$ $\underline{1}$) remained. This comparison of the X-ray data reveals that the (0 0 $\underline{1}$ 0) and (0 0 $\underline{1}$ 4) peak intensities increased with the amount of cold-rolling reduction.

During the superconducting-tape processing, the annealing steps help to heal the fractured particles which result from cold-rolling deformation. In order to study the effect of the annealing temperature on the *c*-axis texture, cold rolled 2223 BSCCO/Ag tape was annealed at various temperatures as shown in Fig. 3. It can be observed that the peak intensities corresponding to the high-T_c phase are maintained up to an annealing temperature of 850 °C, and the strong (0 0 1) reflection is dominant. As the annealing temperature

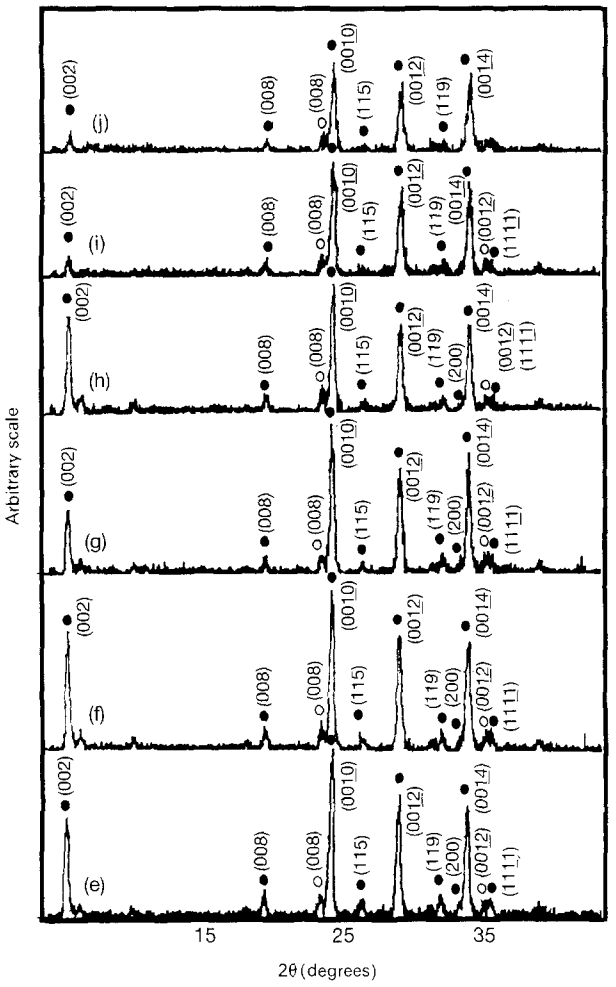

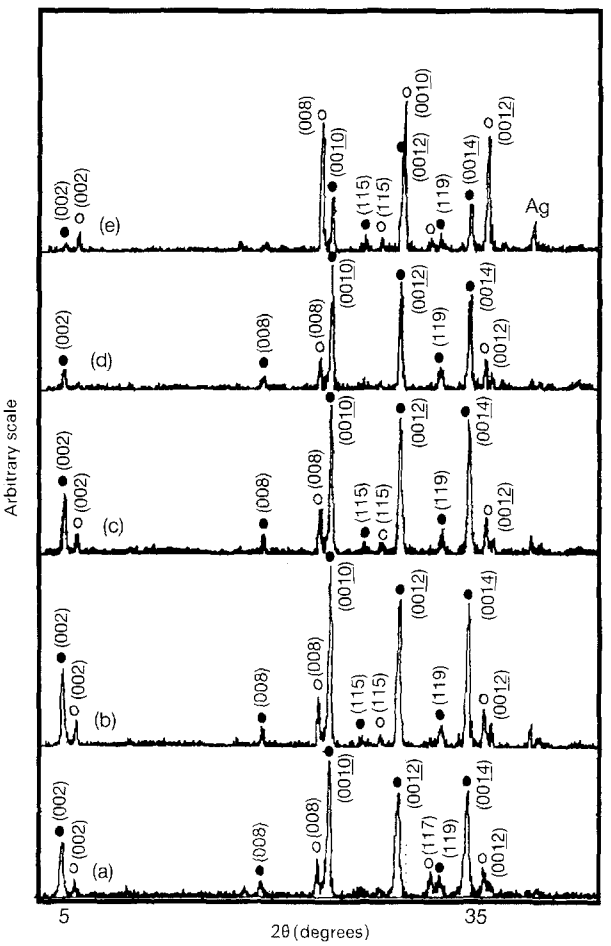

Figure 3 The comparative XRD data for (a) as-rolled (25 μm), and BSCCO/Ag tapes annealed for 5 h at: (b) 830 °C, (c) 840 °C, (d) 850 °C, and (e) 860 °C. (●) High-T_c 2223, and (○) low-T_c 2212.

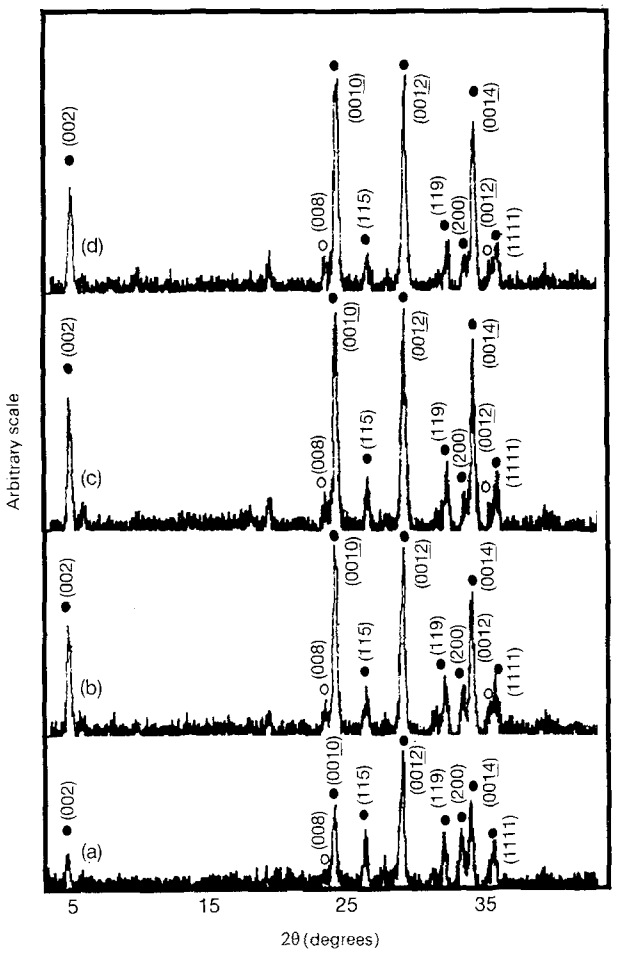

increased to 860 °C, the high-T_c (2223) phase abruptly decomposed into the low-T_c (2212) phase. Normally, the high-T_c (2223) phase is reported to decompose at about 870 °C [11]. This change is presumably due to the lowering of the superconductor melting point by silver [12].

Decomposition of the high-T_c (2223) phase into the low-T_c (2212) phase significantly affects the critical current density (J_c). The 2223 BSCCO/Ag tape which was annealed at 850 °C had a J_c value of 4300 A cm^{-2}, while the 2212 BSCCO/Ag tape which was annealed at 860 °C had a J_c value of 2000 A cm^{-2}, as shown in Fig. 4.

In BSCCO superconductors, long-term annealing or sintering enhances the grain growth of the two-dimensional BSCCO grains. Grain growth is much faster in the *a*- and *b*-directions than in the *c*-direction, so the growing grains assume a plate-like morphology. Actually, it is beneficial to have an annealing texture, if the preferentially oriented grains maintain the pre-alignment resulting from cold-rolling deformation and

Figure 2 The measured XRD data of (a) HIP-cladded Bi/Ag (before rolling); and a successively cold rolled sample with respect to the following cold-rolling-reduction percentages (without annealing) (b) 20%, (c) 30%, (d) 40%, (e) 50%, (f) 60%, (g) 70%, (h) 80%, (i) 90%, and (j) 95%. (●) High-T_c 2223, and (○) low-T_c 2212.

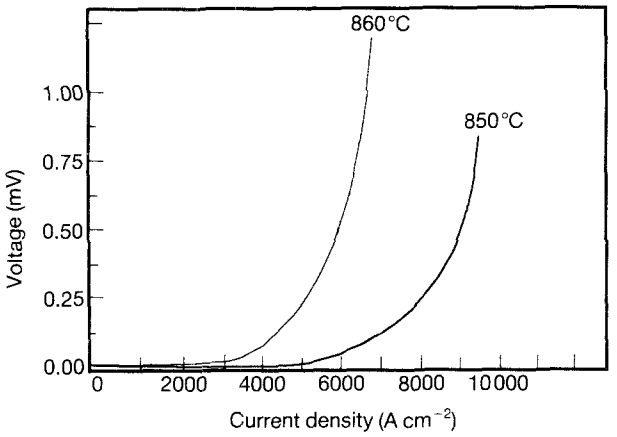

Figure 4 Critical-current-density measurement.

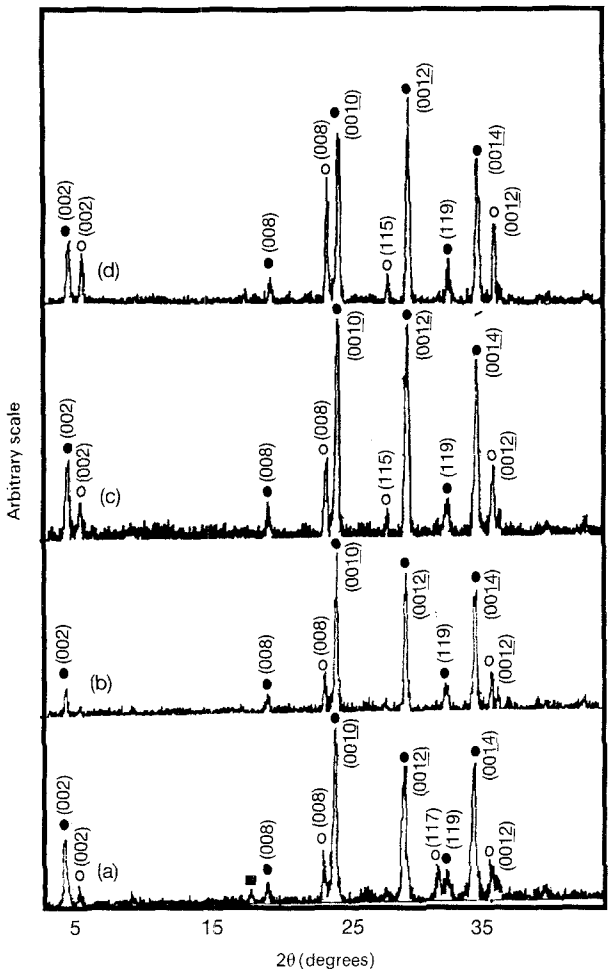

Figure 5 The comparative XRD data for (a) as-rolled (without annealing, 25 μm) BSCCO/Ag tape and for BSCCO/Ag tapes annealed at 850 °C for (b) 5 h, (c) 100 h, and (d) 200 h: (●) High-T_c 2223, (○) low-T_c 2212, and (■) Ca_2PbO_4.

grow larger by consuming some of the smaller misaligned grains. In contrast, it is much more difficult for misoriented grains to grow, since their growth is impeded by the more numerous preferentially oriented grains. However, long-term annealing also promotes gradual decomposition of the high-T_c (2223) phase into the low-T_c (2212) phase, and to non-(0 0 1) grain growth as shown in Fig. 5.

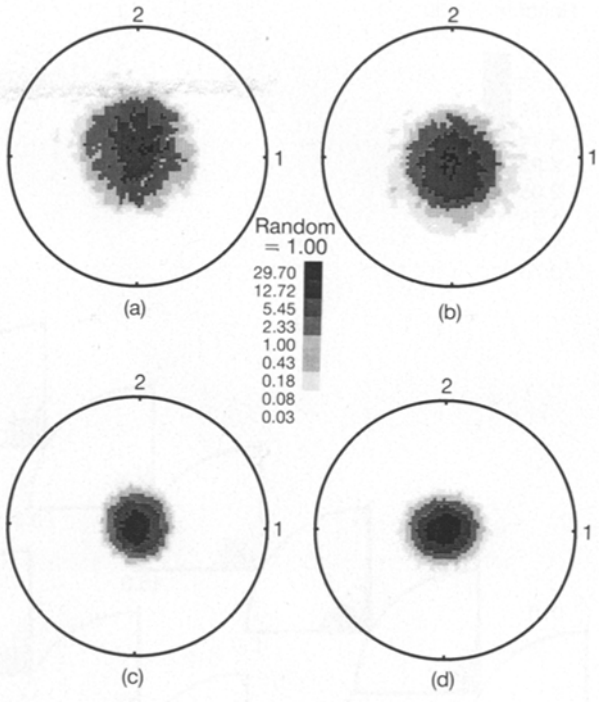

Figure 6 Measured (0 0 1 4) pole figures from a successively rolled and annealed sample: (a) HIP-cladded sample, (b) 20% cold-rolled sample, (c) ~ 99% cold-rolled sample, and (d) a sample annealed at 850 °C for 5 h.

XRD studies, however, do not provide enough information about the precise degree of alignment between the crystal orientations and the preferential orientation with respect to the crystal axes. Such properties are better determined by X-ray pole-figure analysis, since X-ray pole-figure goniometers are designed to measure the diffracted intensity from a sample as it is tilted and rotated to different orientations with respect to the X-ray beam. Experimental (0 0 1 4) pole figures were measured from the initial HIP-cladded surface for different amounts of cold rolling and annealing as shown in Fig. 6. As the amount of cold-rolling reduction increased, a tighter clustering of the (0 0 1 4) poles around the rolling-plane normal indicated that the *c*-axis grains from the initial HIP-cladded surface are reoriented nearly perpendicularly to the plane of the tape. This also suggests that no strong preferential orientation along the rolling and transverse directions exists. From this comparison, the (0 0 1 4) texture is enhanced by the increasing amount of cold rolling; this is consistent with the XRD results.

From the experimental (1 1 5), (1 1 9), and (0 0 1 4) pole-figures, using the popLA software package, which employs harmonic analysis and the Williams–Imhoff–Matties–Vinell (WIMV) method [9], the sample-orientation distribution (SOD) was calculated. The sample orientation distribution (Fig. 7) for a short-term (5 h) annealed sample shows a strong *c*-axis texture, with the *c*-axes aligned perpendicularly to the plane of the tape and no preferred alignment of the *a*- and *b*-axes. (This result shows a good agreement with the microstructural observations (Fig. 11a) for identical sample conditions.) Our preliminary inverse

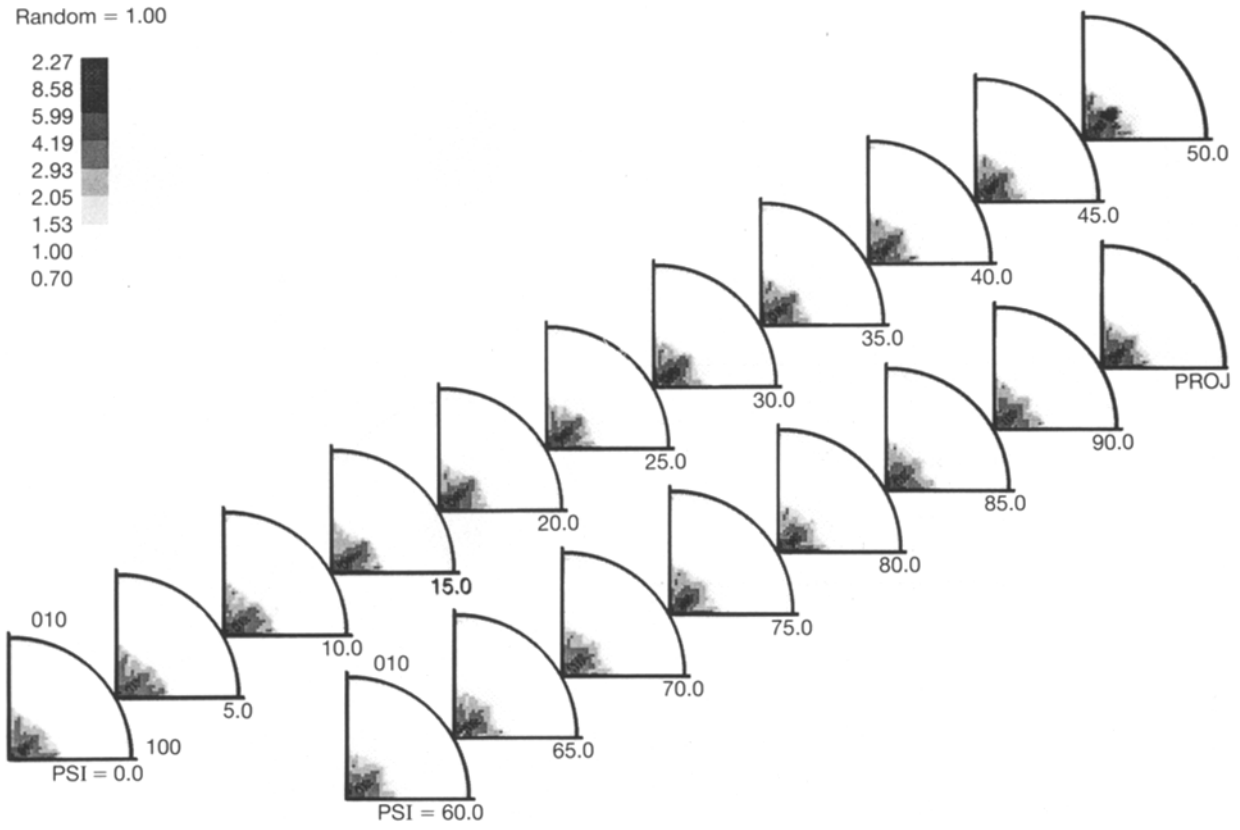

Figure 7 Orientation distribution calculated from pole figures of a sample annealed at 850 °C for 5 h. The last quadrant, PROJ (projection), is the mean of the sections and shows the inverse pole figure for the sample.

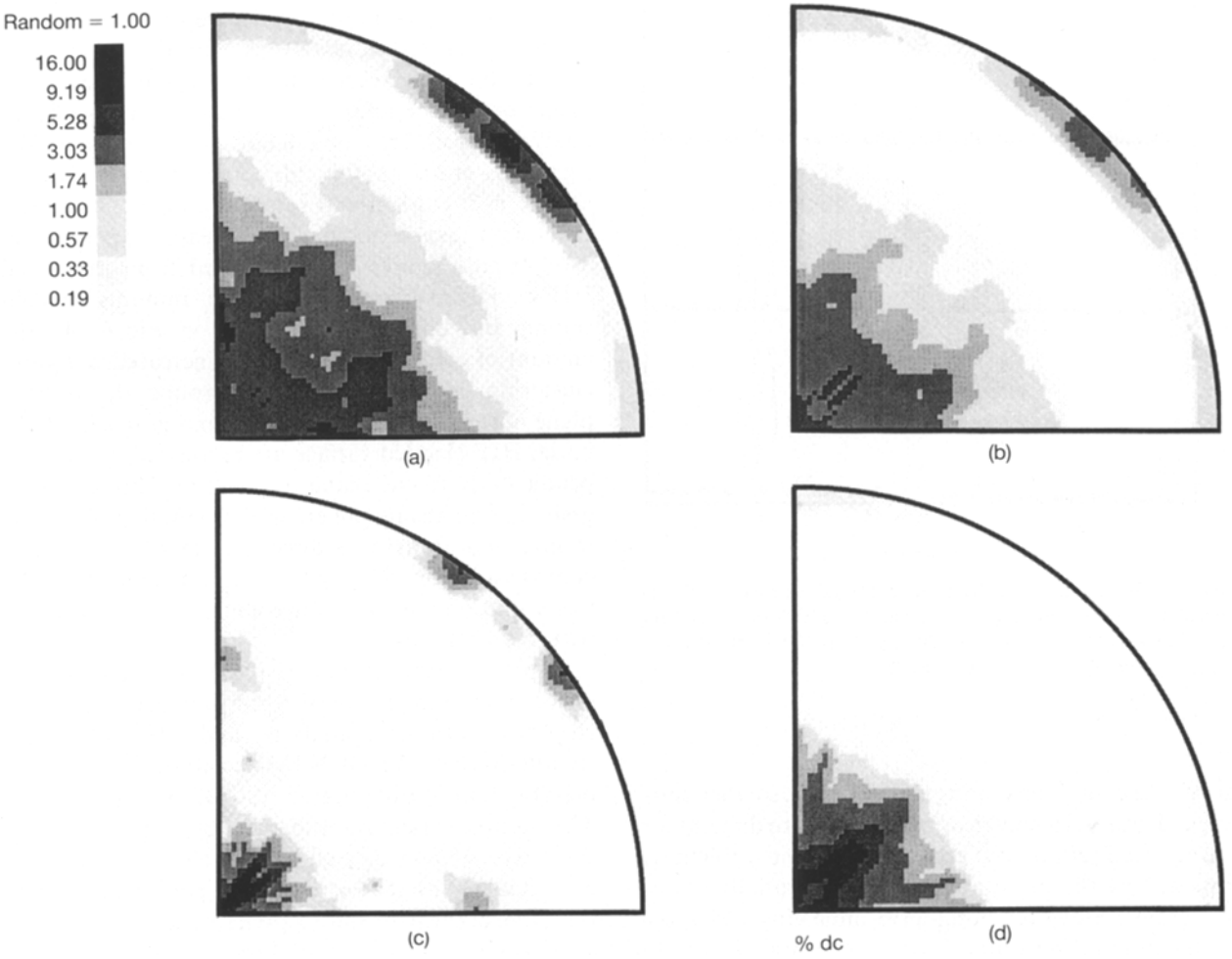

Figure 8 Inverse pole figures for the normal direction calculated from the SOD of the samples for: (a) a HIP-cladded sample, (b) a 20% cold-rolled sample, (c) a ~ 99% cold-rolled sample, and (d) a sample annealed at 850 °C for 5 h.

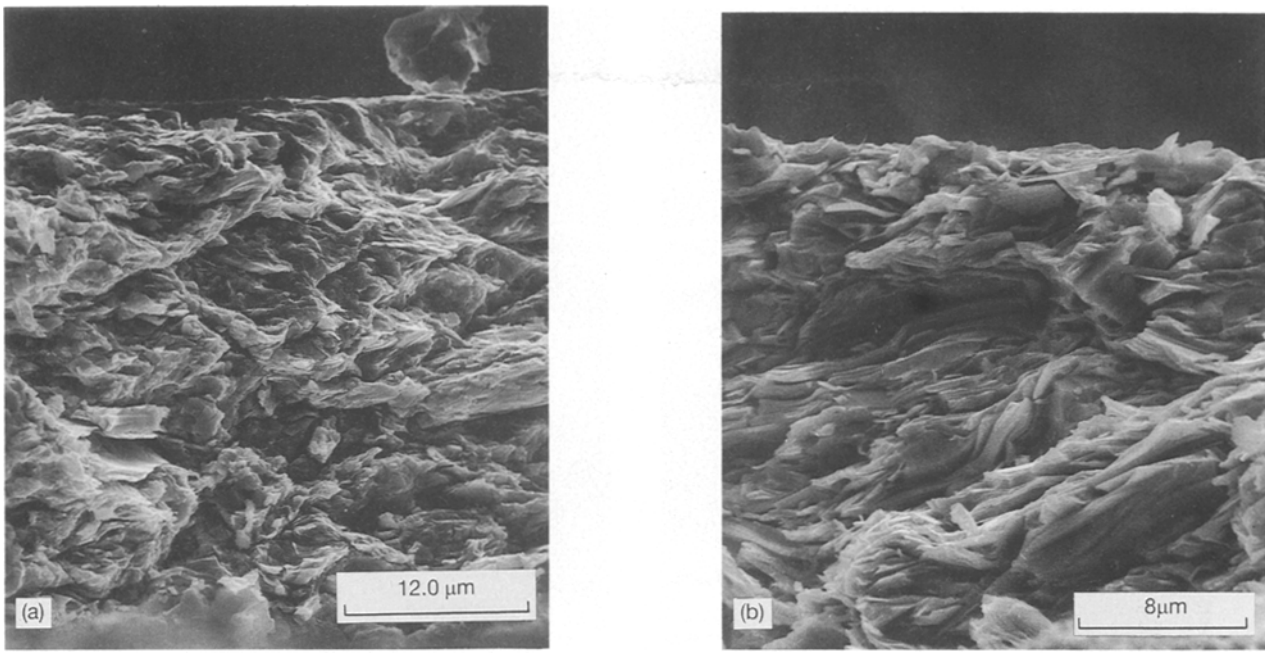

Figure 9 SEM micrographs of fractured longitudinal cross-sections of 2223 BSCCO/Ag tape: (a) as-rolled (without annealing), and (b) annealed at 850 °C for 5 h.

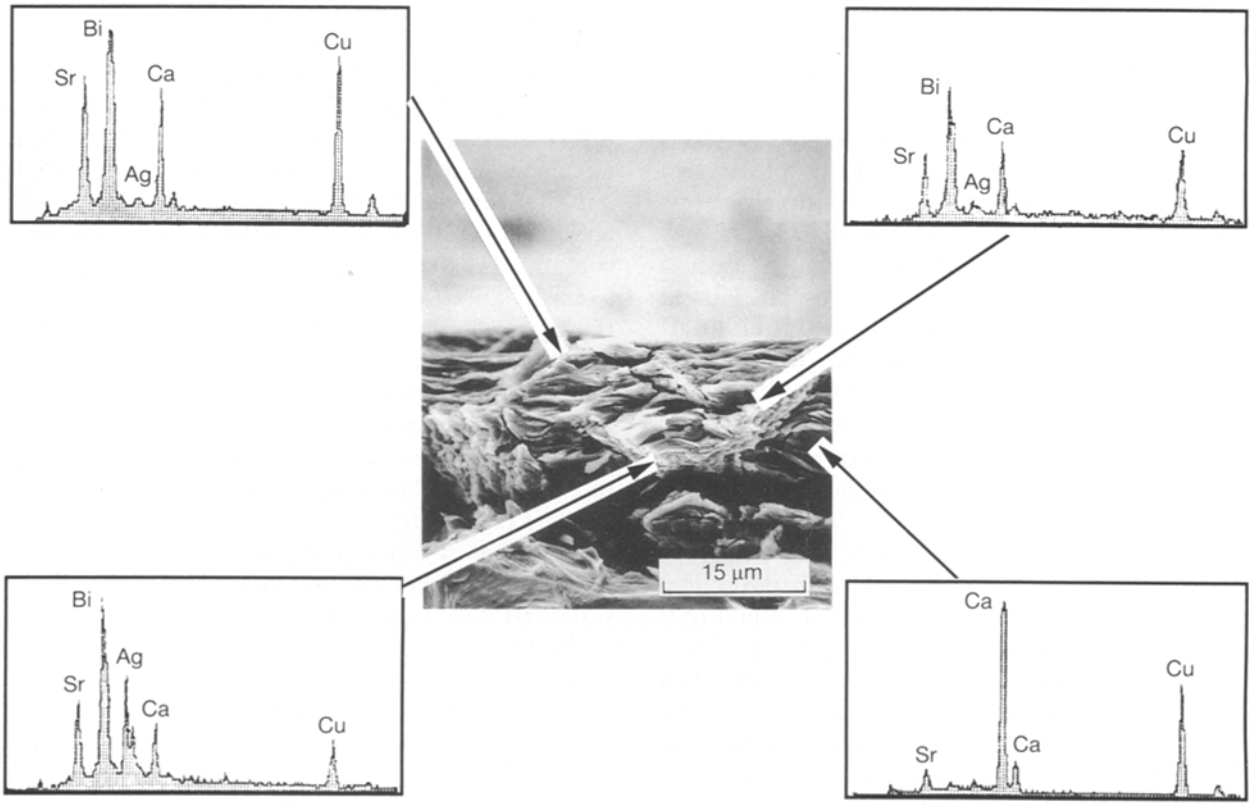

Figure 10 SEM and EDAX of a fractured longitudinal cross-section of BSCCO/Ag tape. The tape was annealed at 850 °C for 100 h.

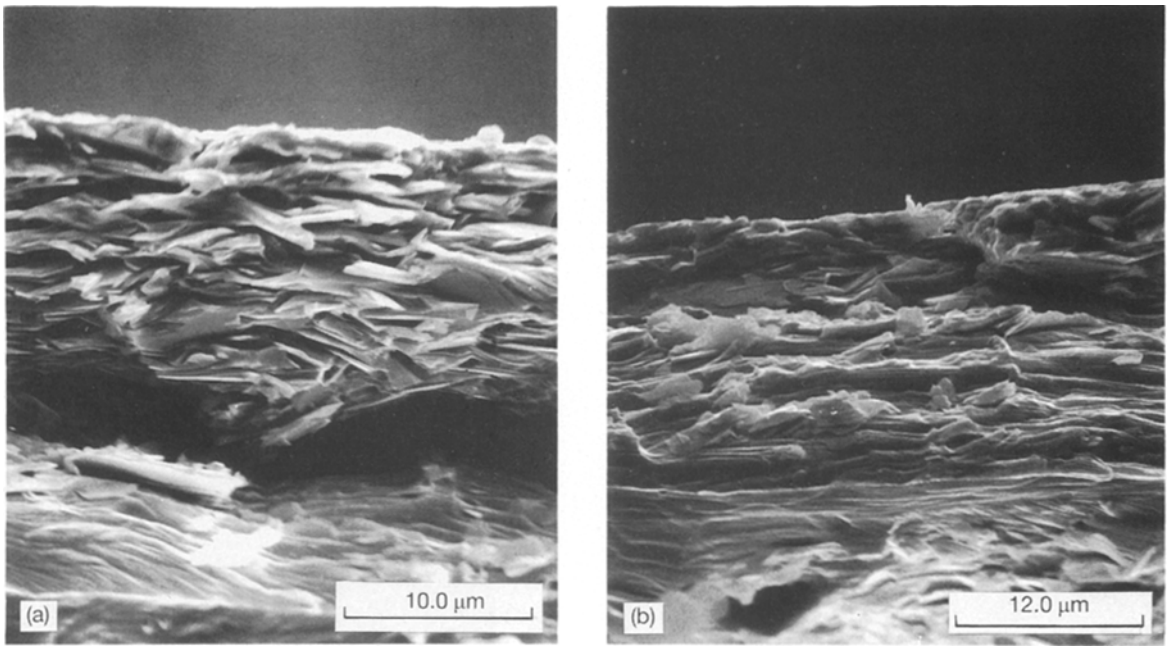

Figure 11 SEM micrographs of fractured longitudinal cross-sections of BSCCO/Ag tape: (a) annealed at 850 °C for 5 h, and (b) annealed at 850 °C for 100 h.

pole-figure data (Fig. 8) reveals that: (i) scattered (0 0 1) grains are oriented nearly perpendicularly to the plane of the tape as the degree of cold rolling increased, and (ii) short term (~ 5 h) annealing caused slight tilting of the (0 0 1) grains.

For the BSCCO superconductor, the possible deformation mechanisms are of two types: (i) a basal-plane system which cleaves easily along the (0 0 1) plane due to the weak structural bonding between two adjacent Bi–O planes [13], and which represents shearing due to dislocation motion, (ii) a lateral system (*a*- and *b*-planes) which may be attributed to sliding following fracture on the *a*- and *b*-planes. Basal slip comprises two systems, (0 0 1) [1 0 0] and (0 0 1) [0 1 0], and lateral slip comprises four possible systems: (1 0 0) [0 1 0], (0 1 0) [1 0 0], (1 0 0) [0 0 1] and (0 1 0) [0 0 1]. According to our experimental pole-figure results, the evolution of a *c*-axis texture during the cold-rolling process strongly supports basal-plane sliding.

We investigated fracture surfaces that were produced by fracturing the tapes parallel to the rolling direction in the thin longitudinal cross-section. Fig. 9 compares scanning electron microscopy (SEM) micrographs of a longitudinal cross-section of a cold-rolled sample and an annealed sample. Well-aligned grains along the rolling direction are reasonably clear. The 2223 BSCCO grain is small and coarsened, which is in agreement with the results of the X-ray data after cold rolling. The fracture morphology of the annealed tape suggests a plate-like grain morphology.

As mentioned above, long-term annealing can significantly enhance the annealing texture, and also slightly promote low-T_c phase conversion and a small amount of non-superconducting-phase formation. SEM and EDAX data of the long-term annealed sample (Fig. 10) suggest that the top surface contains nearly all 2223 phase and very little Ag, while near the Ag interface, the (Ca,Cu)-deficient phase (that is the low-T_c 2212 phase) was found. Some of the darker and rounded grains are the (Ca,Cu)-rich phase, possibly produced by decomposition of the 2223 phase. These conclusions are based on the EDAX analysis.

Fig. 11 compares longitudinal cross-sections of samples annealed for 5 h and 100 h at 850 °C. The (0 0 1) grains are small and slightly tilted from ideal alignment in the 5 h annealed sample. For the 100 h annealed sample, in contrast, the superconductor material near the BSCCO/Ag interface appears to experience more extensive melting. A layer-like growth (*c*-axis texture), which extends macroscopically from the Ag interface is observed. The silver-sheath-induced texture formation may be related to the interaction at the interface with silver, which is known to lower the partial-melting temperature of the BSCCO superconductor and may help to initiate nucleation. Also, recent high-resolution transmission-electron-microscopy (TEM) studies of the 2212 BSCCO/Ag interface suggest that (0 0 1) faceting and 2201 phase were formed at the BSCCO/Ag interface on an atomic scale, and a very strong texturing of the (0 0 1) planes of the BSCCO parallel to the Ag was detected [14]. However, there is still the general question of why the (0 0 1) planes of the 2212 BSCCO phase tend to align macroscopically with the Ag interface. Additional research is required to elucidate the silver-sheath-induced-annealing-texture formation mechanism.

References

1. T. HIKATA, K. SATO, and H. HITOTSUYANAGI, *Jpn. J. Appl. Phys.* **28** (1989) L82.
2. M. UEYAMA, T. HIKATA, T. KATO and K. SATO, *ibid.* **30** (1991) L1384.
3. J. KASE, K. TOGANO, H. KUMAKURA, D. R. DIETDERICH, N. IRISAWA, T. MORIMOTO and H. MAEDA, *ibid.* **29** (1990) L1096.

4. N. ENOMOTO, H. KIKUCHI, N. UNO, H. KUMAKURA, K. TOGANO and N. WATANABE, *ibid.* **29** (1990) L447.
5. G. JIN, J. E. GRAEBNER, T. H. TIEFEL, R. B. VAN DOVER, A. E. WHITE and G. W. KAMMLOTT, *Phisica C.* **177** (1991) 189.
6. Y. TAKEHASHI and T. SUGA, *Jpn. J. Appl. Phys.* **29** (1990) L2006.
7. D. W. JOHNSON and W. W. RHODES, *J. Amer. Ceram. Soc.* **72** (1989) 2346.
8. J. M. YOO and K. MUKHERJEE, *J. Mater. Sci.* **28** (1993) 2361.
9. J. S. KALLEND, U. F. KOCKS, A. D. ROLLET and H. R. WENK, *Mater. Sci. and Engng. A.* **132** (1991) 1.
10. Y. FENG, K. E. HAUTANEN, Y. E. HIGH, D. C. LARBALESTIER, R. RAY II, E. E. HELLSTROM and S. E. BABCOCK, *Phisica C.* **192** (1992) 293.
11. Y. SUZUKI, T. INOVE, S. HAYASHI and H. KOMATSU, *Jpn. J. Appl. Phys.* **28** (1989) L1382.
12. G. KOZLOWSKY, I. MAARTENSE, R. SPYKER, R. LEESE and C. E. OBERLY, *Phisica C.* **173** (1991) 195.
13. E. E. HELLSTROM, *MRS Bull.* August (1992) 45.
14. Y. FENG, D. C. LARBALESTIER, S. E. BABCOCK and J. B. VANDERSANDE, *Appl. Phys. Lett.* **61** (1992) 1234.

Received 18 February
and accepted 24 June 1993